Identification of the catenary structure wavelength using pantograph head acceleration measurements

Wang, Hongrui; Liu, Zhigang; Núñez, Alfredo; Dollevoet, Rolf

DOI
10.1109/I2MTC.2017.7969731

Publication date
2017

Document Version
Accepted author manuscript

Published in
I2MTC 2017 - 2017 IEEE International Instrumentation and Measurement Technology Conference, Proceedings

H. Wang, Z. Liu, A. Núñez, and R. Dollevoet, "Identification of the catenary structure wavelength using pantograph head acceleration measurements". Proceedings of the 2017 IEEE International Instrumentation and Measurement Technology Conference, I2MTC, Torino, Italy, May 22-25, 2017. DOI: 10.1109/I2MTC.2017.7969731

Identification of the Catenary Structure Wavelength using Pantograph Head Acceleration Measurements

Hongrui Wang
Section of Railway Engineering
Delft University of Technology
Delft, the Netherlands
soul_wang0@163.com;
H.Wang-8@tudelft.nl

Zhigang Liu
School of Electrical Engineering
Southwest Jiaotong University
Chengdu, China
liuzg@swjtu.cn

Alfredo Núñez, Rolf Dollevoet
Section of Railway Engineering
Delft University of Technology
Delft, the Netherlands
{a.a.nunezvicencio;
r.p.b.j.dollevoet}@tudelft.nl

***Abstract*— For the condition monitoring of railway catenaries, the potential utilization of pantograph head (pan-head) vertical acceleration instead of pantograph-catenary contact force is discussed in this paper. In order to establish a baseline of the pan-head acceleration before it can be used for health condition monitoring, one of the essential frequency components, namely the catenary structure wavelength (CSW) is studied. Based on in-situ measurements and feature analysis of the pan-head acceleration signal, an adaptive signal filtering approach is proposed to realize the identification of the CSWs. Preliminary results suggest that the CSWs contained in the pan-head acceleration can be reliably identified by the proposed filtering approach.**

Keywords*— *catenary health condition monitoring; pantograph head acceleration; catenary structure wavelength; in-situ measurements; adaptive signal filtering; identification

I. INTRODUCTION

In most of the electrified railways, vehicles receive traction current through the sliding contact between pantograph and catenary above the roof. Due to the intrinsic characteristics of the pantograph-catenary system and various environmental disturbances [1], the contact force between pantograph and catenary fluctuates during operation and determines the current collection quality. Therefore, even expensive, a reliable health condition monitoring technology for the pantograph-catenary system often adopts the contact force as the key measurement parameter to assess the dynamic interaction and eventually the current collection quality [2].

To unify the measurement of contact force in industrial applications, the European Standard EN 50317 specifies the technical requirements [3]. In the standard, the contact force is considered to be composed of the measured contact force F_m, the correction of inertia force F_{ci} and the correction of aerodynamic force F_{ca}. Thus, the final contact force F_C can be calculated by

$$F_C = F_m + F_{ci} + F_{ca}. \quad (1)$$

Consequently, the implementation of the force measurement system requires multiple pressure and acceleration sensors installed on the pantograph. In consideration of the inevitable interferences caused by strong current transmission, pantograph vibration and environmental noise, the technical difficulty and financial cost of the system configuration are both high. As a result, the contact force measurement system is only implemented on a limited number of railway measurement coaches for academic studies and sporadic in-situ tests. For most railway operation companies in the Netherlands only wear and other static parameters are used because to measure the contact force is considered a high investment with low return.

Addressing this cost issue, the pantograph head (pan-head) vertical acceleration has been pointed out to be feasible for catenary condition monitoring as a substitution to the contact force measurement [4]. The pan-head vertical acceleration can reflect the catenary condition for the following two reasons:

1) The inertia force, namely the product of pantograph vertical acceleration and mass, contributes mostly to the fluctuation of contact force. Especially when the train speed is almost constant, the mean contact force and the aerodynamic force will be relatively constant as well. Hence, if the accelerometer is mounted under the pan-head, the measured acceleration will have a correlation with the contact force amplitude [5]. In other words, it preserves the features of the contact force to a certain degree.

2) It is theoretically proven that the pan-head vertical acceleration can reflect the span-passing and dropper-passing frequencies [4], namely the concept of catenary structure wavelengths (CSWs) proposed in [6] that are the dominant and concerned frequencies in the contact force. Hence, the pan-head vertical acceleration can substitute the contact force in similar methodologies for condition monitoring, in which the frequency components are frequently adopted as the indicator of anomalies.

Considering the potential reductions of development cost and technical difficulty, it is promising to employ the pan-head acceleration instead of the contact force in catenary condition monitoring. Hence, in order to accurately apply the pan-head acceleration into practice, basic features of the

This work was supported in part by the National Natural Science Foundation of China under Grant U1434203, 51377136 and 51405401, in part by the Sichuan Province Youth Science and Technology Innovation Team under Grant 2016TD0012, and in part by the China Scholarship Council under Grant 201507000029.

H. Wang, Z. Liu, A. Núñez, and R. Dollevoet, "Identification of the catenary structure wavelength using pantograph head acceleration measurements". Proceedings of the 2017 IEEE International Instrumentation and Measurement Technology Conference, I2MTC, Torino, Italy, May 22-25, 2017. DOI: 10.1109/I2MTC.2017.7969731

acceleration signal must be grasped firstly. Afterwards, the baseline of a specific couple of pantograph-catenary interaction can be established for developing the corresponding detection and diagnosis methods, making possible to facilitate and support the decision of condition-based maintenance. To this end, based on in-situ measurements in the China railway lines, this paper mainly focuses on the analysis and identification of the CSW contained in the pan-head vertical acceleration and presents some preliminary results.

The rest of the paper is organized as follows. The CSW in pan-head vertical acceleration and its relevance with the CSW in contact force are discussed in Section II. The measurement and pre-processing procedures of the pan-head acceleration are introduced in Section III. Section IV illustrates the proposed signal filtering approach that facilitates the identification of CSWs in pan-head acceleration. Finally, conclusions and some future developments are summarized in Section V.

II. THE CSW IN PAN-HEAD ACCELERATION

The CSW is defined as the frequency components that are caused by the cyclic parameter variation of the catenary structure and contained in the pantograph-catenary contact force [6]. As the dominant components in contact force, it plays an important role in the evaluation of current collection quality and anomaly detection. Similarly, because the pan-head acceleration is excited by the catenary structure during the sliding contact with catenary, it is likely to contain the same frequency components. However, since the physical concepts of force and acceleration are by definition different, the CSWs contained in the contact force and the pan-head acceleration are essentially different. In this case, the inertia force, which is proportional to the pan-head acceleration, is actually a part of the contact force. It indicates that there must be a correlation between the contact force and the pan-head acceleration.

Theoretically, at the low-frequency range that contains span-passing and dropper-passing frequencies, the pantograph motion as a whole can be simply described as

$$F_C = F_0 - m\frac{\mathrm{d}^2 y}{\mathrm{d}t^2} = F_0 - ma \tag{2}$$

where F_0 is the sum of static contact force and aerodynamic upward force exerting from the pantograph on the contact wire, t is the time, y is the pantograph vertical displacement and a is the pantograph acceleration as a whole. Assuming under the ideal condition that there is no contact loss in operation, which is true most of the time, the pantograph will always be attached to the contact wire. Although the contact wire height at the contact point, namely the contact point height, is bound to be uplifted by the pantograph sliding contact, the pantograph vertical displacement can still show variations similar to the contact wire height. This is because the stiffness of contact wire changes periodically based on the contact wire height [7]. It can also be seen in in-situ measurement data [8]

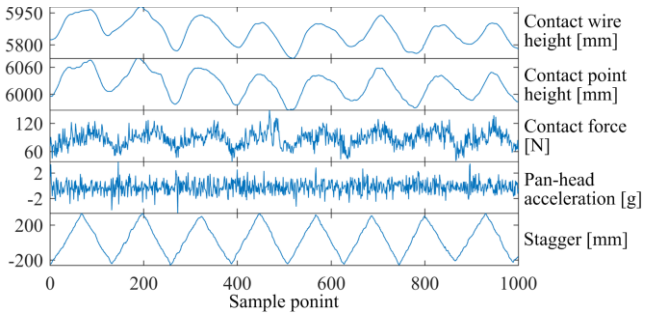

Fig. 1. Example of measurement data set.

that the pantograph height actually follows the static contact wire height. Fig. 1 depicts a set of measurement data from a certain railway line in China. Comparing the contact wire height with the contact point height, the wire is clearly uplifted but the height variation remains highly alike. In addition, when the variation of operation speed is small, the term F_0 in (2) also has a small variation effected by the aerodynamic force only. Since the contact force F_C contains CSWs, the pantograph acceleration a also has the same frequency components but with a phase difference according to the minus sign in (2).

In in-situ measurements, as given in (1), the measured contact force must be corrected by the inertia force F_{ci} that is calculated by

$$F_{ci} = \frac{m_{\text{above}}}{N_a} \cdot \sum_{i=1}^{N_a} a_{sensor,i} \tag{3}$$

where m_{above} is the mass between contact point and sensors, N_a is the number of acceleration sensors and $a_{sensor,i}$ is the acceleration from the ith sensor. In the case that sensors are mounted under the pan-head, m_{above} refers to the mass of pan-head. The pan-head acceleration is the averaged value of all simultaneous measurements when multiple sensors are adopted to reduce errors. It can be seen that the pan-head acceleration is proportional to the inertia force F_{ci}, which directly contributes to the final contact force. Although the amplitude of inertia force may be smaller than the other terms in (1), the variation of inertia force could be considered as an indicator of the contact force variation.

In summary, because the pan-head is excited by the catenary structure in operation, the pan-head acceleration contains frequency components that can reflect the structural parameters. Since these frequencies share the same causes and are similar to the CSWs in contact force, they are hereafter referred as the CSWs in pan-head acceleration.

III. DATA MEASUREMENT AND PRE-PROCESSING

According to the specification in EN 50317 [3] and the majority of previous studies [9-11], a low-pass filter with 20Hz cut-off frequency is prescribed to process the

H. Wang, Z. Liu, A. Núñez, and R. Dollevoet, "Identification of the catenary structure wavelength using pantograph head acceleration measurements". Proceedings of the 2017 IEEE International Instrumentation and Measurement Technology Conference, I2MTC, Torino, Italy, May 22-25, 2017. DOI: 10.1109/I2MTC.2017.7969731

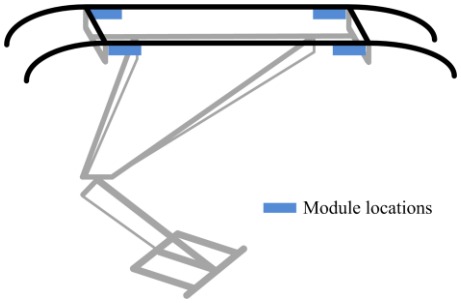

Fig. 2. Sketch of pantograph structure and module locations.

TABLE I
Sensor Parameters

Parameter type	Pressure sensor	Acceleration sensor
Measurement range	0.0~500.0N	±15.00g
Natural frequency	>500Hz	>2000Hz
Measurement accuracy	1%FS	0.2%FS
Maximum overload	1000N	1000g
Maximum sampling frequency	1000Hz	1000Hz

pantograph-catenary contact force data. However, some recent studies noticed that the cut-off frequency is sometimes too low for the purpose of defect detection [4, 12, 13]. Catenary defects such as contact wire irregularity that can excite high frequency response of pantograph can be overlooked by the conventional treatment. Thus, this paper extends the measurement frequency to a fixed sampling interval of 0.5m, i.e. frequencies from 55.6Hz to 166.7Hz under the 100~300km/h range of operation speed.

The different types of data are measured simultaneously by the integrated system configured on a measurement train. Most importantly, there is a pair of integrated sensors, which can measure both pressure and acceleration, attached under each collector on the pan-head. As schematically depicted in Fig.2, the integrated sensor modules are located under both ends of the collectors. Basic parameters of the adopted sensors are described in Table I, where FS denotes the sensor full scale and g is the gravitational acceleration. The results of contact force are corrected as required by (1).

The data set shown in Fig. 1 is measured under the operation speed, about 125 km/h, and de-noised based on tested noise conditions. As mentioned before, the measured signal frequency above 20Hz is expected to be preserved for the benefit of further analysis. Thus, the pan-head acceleration and contact force signals should not be low-pass filtered before they are utilized for specific purposes. To facilitate the identification of CSWs in pan-head acceleration, there are two basic procedures that are to be performed beforehand. The first one is signal segmentation, which ensures that the analysed signal is neither too short to identify the CSWs, nor too long to be frequency-aliasing and time-consuming. The suggested signal length is between 3 and 10 spans of the measured railway line. The second one is removing the mean of signal segment so that frequency identification will not be affected by the non-zero mean. Note that the order of the two

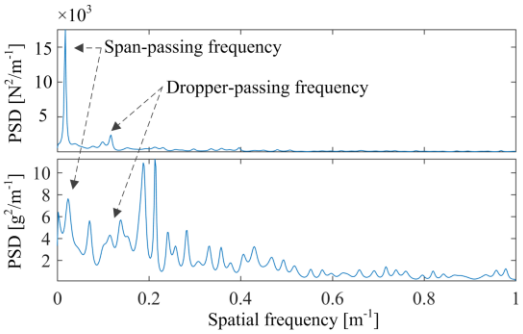

Fig. 3. PSDs of contact force (above) and pan-head acceleration (below).

procedures cannot be altered; otherwise, the mean of signal segment cannot be correctly eliminated.

IV. Identification of CSWs in Pan-Head Acceleration

Aside from the CSWs, other frequency components contained in the pan-head acceleration are certainly different from those in the contact force. The pantograph-head vibration contains much complex high-frequency components that can hardly be reflected by the contact force. In particular, the deformable modes of the collector normally occupy a considerable portion of energy in pantograph vibrations [13]. In some cases, they are observed as the dominant frequencies in pan-head acceleration instead of the CSWs [4]. This brings up a major challenge for the identification of CSWs that is avoiding the submergence and contamination of other frequencies.

Concretely, Fig. 3 depicts the power spectral densities (PSDs) of the pan-head acceleration and contact force signals presented in Fig. 1. The length of the signals is about 8 spans, which meets the aforementioned requirement. It can be seen that the PSD of contact force is relatively smooth with only two peaks at span-passing and dropper-passing frequencies, namely the CSWs. Meanwhile, the PSD of pan-head acceleration clearly reflects multiple frequency components, including the CSWs as indicated by the dashed lines in Fig. 3. However, the other components with high spectral amplitude and adjacent frequency could disturb the identification of CSWs. Especially the components with spatial frequency close to $0.2m^{-1}$, they can easily be mixed with the dropper-passing frequency that commonly lies between $0.1m^{-1}$ and $0.2m^{-1}$.

In our previous study, the identification of CSWs in contact force is realized based on the ensemble empirical mode decomposition (EEMD) [6]. For the CSWs in pan-head acceleration, considering the interferences caused by the non-CSW part of the signal, some alterations are required to improve the identification results. The direct solution would be filtering out the frequencies outside of the potential frequency range of CSWs. Under the operation speed around 125km/h, this frequency range lies between $0.014m^{-1}$ and $0.025m^{-1}$ concerning the spans, and between $0.1m^{-1}$ and $0.2m^{-1}$ concerning the interdropper distances. To identify the CSWs

while eliminating the influences of adjacent frequencies, the following method based on EEMD is proposed.

A. *EEMD*

The predecessor of EEMD, namely the empirical mode decomposition (EMD), has been noticed for its potential in signal filtering from a decade ago [14]. It adaptively decomposes a signal into several intrinsic mode functions (IMFs) that possess diminishing frequency bands. These IMFs are generated from the signal itself without introducing any additional basic signals. Thus the inherent physical significance of IMFs is considered as the major advantage of EMD algorithm.

EEMD is basically the improved EMD with the physical significances enhanced by resolving the mode mixing problem [15]. This is particularly important for the identification of CSWs. As structure-induced frequencies, the CSWs are not constant in many cases. For various railway lines, the CSWs are different since the structural parameters of catenary are normally different. Even for the same railway line, the catenary structure may change along the entire line. Furthermore, if the operation speed changes during operation, the frequencies of CSWs will be different too. Theoretically, all the aforementioned issues can be addressed by the EEMD. No matter how the frequencies may deviate in different cases, EEMD can preserve these frequencies because it automatically adapts to the frequency deviations.

The EEMD algorithm can be briefly described in four steps.

Step 1: Add a white noise series to the original signal $x(t)$ to form a new and contaminated signal.

Step 2: Perform the EMD [16] on the new signal and obtain a set of IMFs.

Step 3: Repeat *Step 1* and *Step 2* M times.

Step 4: Output the final IMFs by averaging the corresponding IMF in the M sets of IMFs.

After the signal $x(t)$ is decomposed into a number N of IMFs $d_j(t)$, $j=1,2,\ldots,N$ and a residual $r(t)$ by the EEMD, the signal can be reconstructed as

$$x(t)=\sum_{j=1}^{N} d_j(t)+r(t). \tag{4}$$

B. *EEMD-based Filtering and Identification*

As an example, the decomposed results of the pan-head acceleration in Fig. 1 are depicted in Fig. 4. There are nine IMFs extracted from the acceleration signal in total. From the corresponding PSDs of IMFs on the right of Fig. 4, it can be seen that the frequency band of IMFs declines from the first to the ninth one. Because the CSWs is normally lower than 0.2m^{-1}, the required signal filtering can simply be done by subtracting the IMFs with higher frequency. Judging from the PSDs, the frequency bands of the second and third IMFs have certain overlap with the spatial frequency 0.2m^{-1}. To quantify

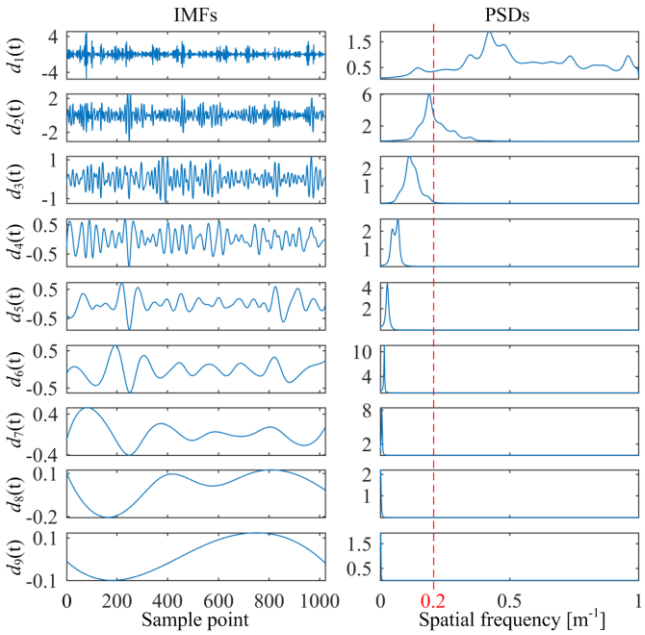

Fig. 4. IMFs of the pan-head acceleration (left) and the corresponding PSDs (right).

the overlap and thus decide if the IMF should be included or excluded from the filtered signal, the following index is proposed

$$I_j=\mathrm{sgn}(f_c-\arg\max_f[P_j(f)])\cdot\frac{P_j(f_c)}{\max[P_j(f)]} \tag{5}$$

where $P_j(f)$ is the PSD of the jth IMF, f_c is the threshold for the identification of CSWs and typically 0.2m^{-1}, $\arg\max_f[P_j(f)]$ denotes the arguments of the maximum $P_j(f)$, sgn[·] is the sign function and max[·] is the maxima function.

Based on the index defined by (5), the jth IMF can be considered as below 0.2m^{-1} in the frequency domain and included in the filtered signal if $I_j \geq 0.1$. Specifically, the sign function in (5) is used to judge that, if the maximum energy of PSD is located at a frequency higher than the threshold f_c, namely the sign function outputs -1, the IMF cannot be recognized as possible CSW; otherwise, it is possible that the IMF belongs to CSWs. The fraction part of (5) is actually constrained by the sign function and only contributing when the sign function outputs 1. It describes the proximity of the spectral energy at the threshold f_c to the maximum energy. When it is lower than 0.1, the corresponding IMF is considered as not significant enough to be the CSWs. To sum up, the procedures of proposed filtering approach for the purpose of CSWs identification are summarized in Fig. 5.

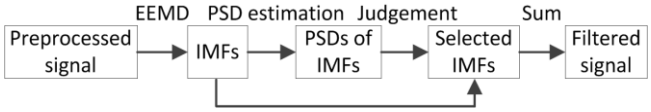

Fig. 5. Procedures of the EEMD-based filtering approach.

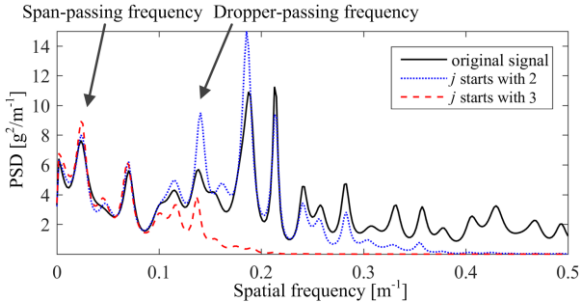

Fig. 6. PSDs of the orginal pan-head acceleration and filtered signals.

According to the index and PSDs in Fig. 4, the filtered signal $x_c(t)$ in this case can be constructed excluding the first two IMFs as

$$x_c(t) = \sum_{j=3}^{N} d_j(t) + r(t) . \quad (6)$$

From the frequency perspective, comparisons between the original signal and the filtered signals constructed by (4) when j starts with 2 and 3 are respectively depicted in Fig. 6. The filtered signal determined by the index in (5) is drawn with dashed line, while the original signal is drawn with solid line and the other filtered signal is drawn with dotted line. It can be seen that comparing with the original signal, the CSWs indicated by arrows are revealed with the EEMD-based filtering. But, the filtering results in the case that j starts with 2 still contains significant spectral energy at spatial frequencies higher than 0.2m^{-1}, which is beyond the reach of CSWs. Thus, the filtering result in the case that j starts with 3 should be adopted for the identification of CSWs in pan-head acceleration. By means of the adaptive filtering approach, the CSWs can be clearly identified in the filtered signal. Comparing with the traditional low-passing filtering technique, the proposed filtering approach can realize the identification of CSWs in pan-head acceleration with the following two unique advantages:

1) It automatically adapts to the common frequency deviations of CSWs in measurements. There is no need to adjust the filtering approach for different scenarios.

2) All the information is contained in the original signal and it will not be damaged by filtering, because the signal is decomposed based on the physical components rather than be cut off with a fixed frequency boundary.

V. Conclusion and Future Work

Aiming at establishing a baseline for the application of pan-head acceleration in catenary condition monitoring, this paper studies one of the basic features of pan-head acceleration. The CSWs in pan-head acceleration, which are the essential low-frequency response of pan-head, and its differences with the CSWs in contact force are introduced and discussed. The identification of CSWs is realized by the adaptive signal filtering that combines the EEMD algorithm with a new judgement index based on PSD. The identified CSWs in pan-head acceleration can be used as an indicator for the evaluation of current collection quality and the structural parameter deviation of catenary.

Moreover, if the CSWs in pan-head acceleration can be properly eliminated, the residual of pan-head acceleration will be a better candidate for detecting and diagnosing the defects of catenary and anomalies existed in pantograph-catenary interaction. In the future, the frequency range for pan-head acceleration measurement should be further expanded to around 100Hz or higher. Thus, essential frequency components such as the deformable modes of pantograph collector can be treated in a similar manner to the CSWs, so that the baseline of pan-head acceleration can be established.

References

[1] A. Collina, F. Fossati, M. Papi, and F. Resta, "Impact of overhead line irregularity on current collection and diagnostics based on the measurement of pantograph dynamics," Proc. IMechE Part F: J. Rail Rapid Transit, vol. 221, no. 4, pp. 547-559, 2007.

[2] H. Wang, Z. Liu, Y. Song, X. Lu, Z. Han, J. Zhang, and Y. Wang, "Detection of contact wire irregularities using a quadratic time-frequency representation of the pantograph-catenary contact force," IEEE Trans. Instrum. Meas., vol. 65, no. 6, pp. 1385 - 1397, Jun. 2016.

[3] Railway Applications—Current Collection Systems—Requirements for and Validation of Measurements of the Dynamic Interaction Between Pantograph and Overhead Contact Line, document BS EN 50317, GEL/9/3, 2012.

[4] M. Carnevale and A. Collina, "Processing of collector acceleration data for condition-based monitoring of overhead lines," Proc. IMechE Part F: J. Rail Rapid Transit, DOI:10.1177/0954409714545637.

[5] S. Kusumi, T. Fukutani, and K. Nezu, "Diagnosis of overhead contact line based on contact force," Quart. Rep. of RTRI, vol. 47, no. 1, pp. 39-45, Feb. 2006.

[6] Z. Liu, H. Wang, R. Dollevoet, Y. Song, A. Núñez, and Jing Zhang, "Ensemble EMD-based automatic extraction of the catenary structure wavelength from the pantograph–catenary contact force," IEEE Trans. Instrum. Meas., vol. 65, no. 10, pp. 2272-2283, Oct. 2016.

[7] Y. Song, Z. Liu, H. Wang, X. Lu, and J. Zhang, "Nonlinear modelling of high-speed catenary based on analytical expressions of cable and truss elements," Veh. Syst. Dyn., vol. 53, no. 10, pp. 1455-1479, Jun. 2015.

[8] S. Harada and S. Kusumi, "Monitoring of overhead contact line based on contact force," The IET international conference on railway condition monitoring, pp. 188-193, Nov. 2006.

[9] A. Facchinetti and M. Mauri, "Hardware-in-the-loop overhead line emulator for active pantograph testing," IEEE Trans. Ind. Electron., vol. 56, no. 10, pp. 4071-4078, Oct. 2009.

[10] P. Boffi, G. Cattaneo, L. Amoriello, A. Barberis, G. Bucca, M. Bocciolone, et al, "Optical fiber sensors to measure collector performance in the pantograph-catenary interaction," IEEE Sensors Journal, vol. 9, no. 6, pp. 635-640, Jun. 2009.

[11] S. Bruni, J. Ambrosio, A. Carnicero, Y. H. Cho, L. Finner, M. Ikeda, S. Y. Kwon, J. Massat, S. Stichel, M. Tur, and W. Zhang, "The results of the pantograph–catenary interaction benchmark," Veh. Syst. Dyn., vol. 53, no. 3, pp. 412-435, Jun. 2015.

[12] M. Bocciolone, G. Bucca, A. Collina, and L. Comolli. "An approach to monitor railway pantograph-catenary interaction with fiber optic sensors," Proc SPIE, vol. 7653, pp. 76533Q-1-76533Q-4, 2010.

[13] A. Collina, A. L. Conte, and M. Carnevale, “Effect of collector deformable modes in pantograph—catenary dynamic interaction,” Proc. IMechE Part F: J. Rail Rapid Transit, vol. 223, no. 1, pp. 1-14, Jan. 2009.

[14] P. Flandrin, G. Rilling, and P. Goncalves, “Empirical mode decomposition as a filter bank,” IEEE Signal Process. Lett., vol. 11, no. 2, pp. 112-114, Feb. 2004.

[15] Z. Wu and N. E. Huang, “Ensemble empirical mode decomposition: A noise-assisted data analysis method,” Adv. Adapt. Data Anal., vol. 1, no. 1, pp. 1–41, 2008.

[16] N. E. Huang *et al.*, “The empirical mode decomposition and the Hilbert spectrum for nonlinear and non-stationary time series analysis,” Proc. Roy. Soc. London A, vol. 454, pp. 903–995, Mar. 1998.